Advection flow effects in the growth of a free dendrite

Massimo Conti
Dipartimento di Fisica, Universitá di Camerino and Istituto Nazionale di Fisica della Materia, Via Madonna delle Carceri, I-62032 Camerino, Italy

(Received 29 April 2003; revised manuscript received 21 October 2003; published 17 February 2004)

The growth of a free dendrite into a supercooled liquid is simulated through a modified version of the phase-field model, which takes into account the advection flow due to the different densities ρ_s and ρ_l of the solid and liquid phases. The intensity of the flow is maximal at the dendrite tip and decays far from the surface of the crystal. At fixed undercooling, as the density ratio ρ_s/ρ_l increases, we observe a decrease of the tip velocity, while the tip radius increases. The Peclet number is shifted with respect to the pure diffusive value. The onset of the morphological instability, which is responsible for the origin of the dendrite from a growing circular germ, is slightly anticipated by the flow effects.

DOI: 10.1103/PhysRevE.69.022601 PACS number(s): 81.10.Mx, 05.70.Fh, 64.70.Dv, 05.70.Ln

Most theoretical models for dendritic solidification assume a pure diffusive mechanism for the latent heat released at the solid-liquid interface. The steady solution obtained by Ivantsov [1] for a free dendrite is a shape-preserving parabola which can be characterized by the tip radius $R_{\rm tip}$ and the velocity $v_{\rm tip}$. Ivantsov's analysis fixes the product of these quantities, through a relation between the Peclet number $P=R_{\rm tip}v_{\rm tip}/2D$ (D is the thermal diffusivity) and the dimensionless supercooling imposed at infinity $\Delta=C(T_0-T_\infty)/L_0$, where C is the specific heat, T_0 represents the coexistence temperature of the solid and liquid phases, and L_0 the latent heat per unit mass. The degeneracy of this solution was removed observing that for a stable and steady tip propagation an anisotropic surface tension γ is required, and the dendrite operating point was identified determining the value of the so called stability constant $\sigma^*=d_0D/(R_{\rm tip}^2v_{\rm tip})$, where $d_0=(\gamma C T_0)/(\rho_0 L_0^2)$ is the capillary length [2]. However, in most solidification experiments a convection flow arises in the melt. Even in the absence of buoyancy effects (i.e., in space experiments [3]) anomalies in dendritic growth were observed, which were ascribed to the advection flow driven by the density change in the liquid-solid transition. McFadden and Coriell [4] extended the free-boundary diffusive model to incorporate the advection effects, obtaining two main results: (i) a parabolic shape is still consistent with a steady growth of the dendrite, and (ii) the Peclet number depends not only on the melt's undercooling, but it is also a decreasing function of the density ratio $S=\rho_s/\rho_l$. In this paper we address the coupled thermal and hydrodynamic problem for the growth of a free dendrite using a modified version of the phase-field model [5], which incorporates previous ideas proposed by Caginalp and Jones [6], Oxtoby [7], Anderson *et al.* [8], and Tong *et al.* [9]. The numerical solution of the model shows that in the early stage of the growth, the sudden dilatation (or compression) of the liquid in front of the interface originates pressure (and density) waves that propagate into the sample. Even before the relaxation of this mechanical transient a needle crystal is formed, with a well defined tip radius and velocity. At fixed undercooling, as the density ratio S increases, we observe a decrease of the tip velocity, while the tip radius increases, and the Peclet number deviates from the pure diffusive value. The onset of the morphological instability is slightly anticipated by the flow effects. The derivation of the governing equations is presented in detail in Ref. [5]. The order parameter ϕ takes the value $\phi=0$ in the solid and $\phi=1$ in the liquid. The solid phase is modeled as an isotropic fluid with large viscosity. We indicate with T_0, p_0, ρ_{s0}, and ρ_{l0} the temperature, pressure, solid, and liquid density, respectively, in an equilibrium reference state. The equilibrium density $\rho_0(\phi)$ is assumed to change in the interfacial region as $\rho_0\equiv\rho_0(\phi)=\rho_{s0}+p(\phi)(\rho_{l0}-\rho_{s0})$, where the function $p(\phi)=\phi^3(10-15\phi+6\phi^2)$ is monotonic and increasing with ϕ, taking the values $p(0)=0$, $p(1)=1$. A nondimensional form of the model equations is obtained adopting a reference length ξ and scaling time to $\tau=\xi^2/D$. Density is scaled as ρ/ρ_{l0} and a nondimensional temperature is introduced as $u=C(T-T_0)/L_0$. Specific energies will be scaled to v_0^2, where $v_0=\xi/\tau$, and the scale for the components of the stress tensor is $\rho_{l0}v_0^2$. Notice that in the following we neglect thermal expansion effects; moreover, equal values in both phases are assumed for the specific heat, the thermal diffusivity, and the isothermal compressibility.

Then, the model equations read

$$\frac{d\rho}{dt}=-\rho\vec{\nabla}\cdot\vec{v}, \tag{1}$$

$$\rho\frac{d\vec{v}}{dt}=\nabla\cdot(\mathbf{T}+\mathbf{\Pi}), \tag{2}$$

$$\frac{du}{dt}+p'(\phi)\frac{d\phi}{dt}=\nabla^2u+\frac{1}{\rho R_5}(\mathbf{\Pi}:\nabla\vec{v}), \tag{3}$$

$$\frac{d\phi}{dt}=m\left\{\vec{\nabla}\cdot[\eta^2(\theta)\vec{\nabla}\phi]+\frac{\partial}{\partial y}[\eta(\theta)\eta'(\theta)\phi_x]-\frac{\partial}{\partial x}[\eta(\theta)\eta'(\theta)\phi_y]\right\}-\frac{m}{\tilde{\epsilon}^2}\left[\frac{\partial g(\phi)}{\partial\phi}-p'(\phi)\rho\alpha\tilde{\epsilon}u\right]-\frac{1}{2}p'(\phi)\rho(1-S)R_1\left(\frac{\rho_0^2-\rho^2}{\rho^2\rho_0^2}\right), \tag{4}$$

where **T** and **Π** indicate, respectively, the capillary and the viscous stress tensor, whose components are

$$T_{xx} = -p_0 - \frac{R_1 R_3}{m}\frac{(\rho-\rho_0)}{\rho} + R_2\rho_y^2 + R_3\phi_y^2,$$

$$T_{yy} = -p_0 - \frac{R_1 R_3}{m}\frac{(\rho-\rho_0)}{\rho} + R_2\rho_x^2 + R_3\phi_x^2,$$

$$T_{xy} = T_{yx} = -R_2\rho_x\rho_y - R_3\phi_x\phi_y,$$

$$\Pi_{xx} = R_4\lambda(\phi)\left(\frac{4}{3}\frac{\partial v_x}{\partial x} - \frac{2}{3}\frac{\partial v_y}{\partial y}\right) + R_7\nabla\cdot\vec{v},$$

$$\Pi_{yy} = R_4\lambda(\phi)\left(\frac{4}{3}\frac{\partial v_y}{\partial y} - \frac{2}{3}\frac{\partial v_x}{\partial x}\right) + R_7\nabla\cdot\vec{v},$$

$$\Pi_{xy} = \Pi_{yx} = R_4\lambda(\phi)\left(\frac{\partial v_x}{\partial y} + \frac{\partial v_y}{\partial x}\right). \tag{5}$$

In the above equations the parameters are defined as

$$m = \frac{\mu\gamma T_0}{D\rho_{l0}L}, \quad \tilde{\epsilon} = \frac{h}{\xi}, \quad \alpha = \frac{\xi}{6\sqrt{2}d_0},$$

$$R_1 = \frac{\mu\tau T_0}{6\sqrt{2}hk\rho_{l0}L}, \quad R_2 = R_3 = \frac{6\sqrt{2}\gamma h}{\xi^2\rho_{l0}v_0^2},$$

$$R_4 = \frac{\eta_l}{\tau\rho_{l0}v_0^2}, \quad R_5 = \frac{L_0}{v_0^2}, \quad R_7 = \frac{\zeta_l}{\tau\rho_{l0}v_0^2}, \tag{6}$$

where h is the interface thickness and μ is the kinetic undercooling coefficient that relates the interface undercooling to the interface velocity v_I through $v_I = \mu(T_0 - T)$; k is the isothermal compressibility and η_l, ζ_l represent the first and second viscosity in the liquid. The function $g(\phi) = (1/4)\phi^2(1-\phi)^2$ is the classic double well Landau-Ginzburg contribution to the free energy. Anisotropy of the surface energy is accounted for through the function $\eta(\theta) = (1+\omega\cos 4\theta)$, where θ is defined as the angle between the normal to the interface and a fixed direction, the x axis in our calculations, and ω specifies the intensity of the anisotropy. The function $\lambda(\phi)$ describes the transition of the system's viscosity across the interface. In the bulk solid we assumed $\eta_s = 10^3\eta_l$. To allow a complete relaxation of the order parameter towards the stable solid phase in a reasonable time, we defined $\lambda(\phi) = \eta_s/\eta_l + q(\phi)(1-\eta_s/\eta_l)$ with $q(\phi) = 1$ for $\phi \geqslant 0$ and $q(\phi) = 0$ for $\phi = 0$. For the thermophysical properties we referred to the data of nickel. However, due to limitations of computational resources, a compressibility value has been chosen, resulting in a sound velocity that is one order of magnitude lower than the actual value. The interface thickness has been chosen as $h = 50\times10^{-8}$ cm. With a length scale $\xi = 2\times10^{-4}$ cm, we have the following values of the model parameters: $\alpha = 265$, $m = 0.1$, $\tilde{\epsilon} = 2.5\times10^{-3}$, $\omega = 0.02$, $R_1 = 2.12\times10^4$, $R_2 = R_3 = 1.78\times10^{-2}$, $R_4 = R_7 = 0.105$, $R_5 = 4.94\times10^3$, $\Delta = 0.7$.

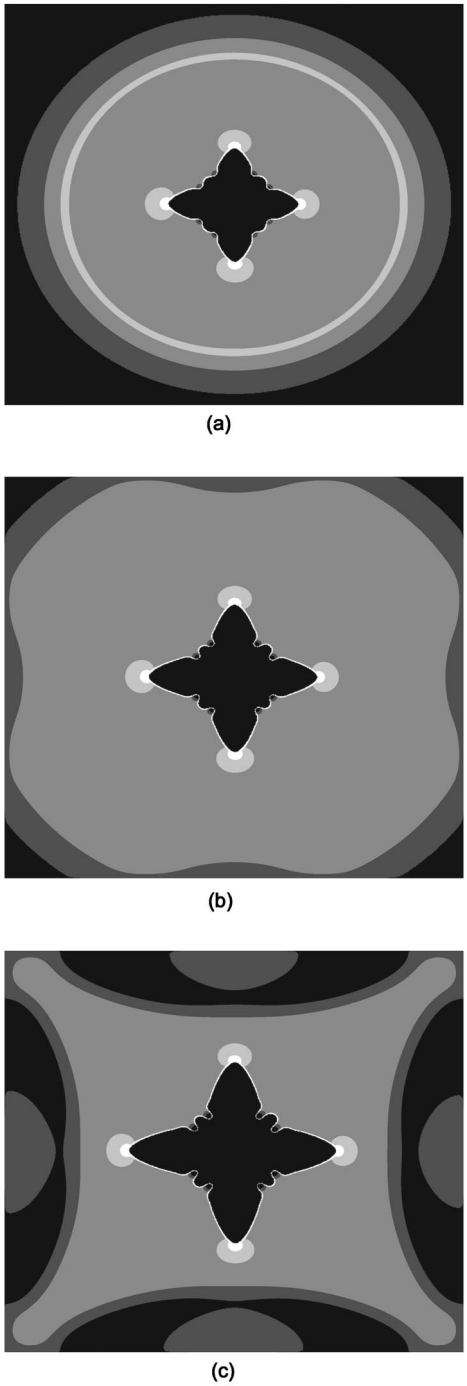

FIG. 1. The pressure wave originated at the solid-liquid interface, at times 2.43×10^{-2} (a), 3.24×10^{-2} (b), and 4.05×10^{-2} (c). The density ratio is $S = 1.05$. In order of increasing darkness the five zones represent pressure values $-25 \leqslant p \leqslant -20$, $-20 \leqslant p \leqslant -15$, $-15 \leqslant p \leqslant -5$, $-5 \leqslant p \leqslant -0.1$, $-0.1 \leqslant p \leqslant 0$.

Equations (1)–(4) have been solved on a computational domain $0 \leqslant x \leqslant x_m$, $0 \leqslant y \leqslant y_m$, with $x_m = y_m = 3.75$. Neumann boundary conditions were imposed at the domain's borders. Time integration was exploited through an explicit scheme except for the momentum equations, in which, due to the large viscosity of the solid phase, we were forced to employ an implicit scheme. Second-order central differences

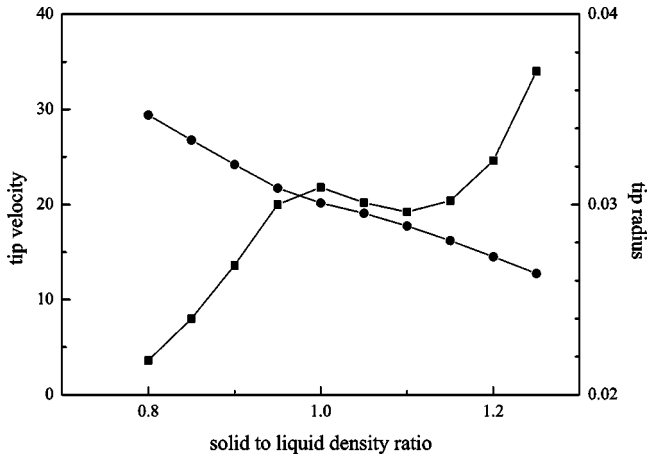

FIG. 2. The tip velocity (dots) and the tip radius (squares) vs the density ratio S.

were used for the Laplace operator, and upwind differences for the convective terms. The grid spacing was selected as $\Delta x=\Delta y=\tilde{\epsilon}$; the time step required for numerical stability is $\Delta t=1.0\times10^{-6}$. Following a standard method in computational fluid dynamics, the velocity fields v_x, v_y were solved on two computational grids shifted $\Delta x/2$ and $\Delta y/2$ in respect to that used for the scalar fields.

Initially, the melt is at rest, at uniform temperature $u=-\Delta$; then a circular solid germ is nucleated at the center of the domain, with a supercritical radius $R_0=0.04$. In the first stage of the growth, surface tension effects prevail, resulting in a circular shape of the crystal; then, after the onset of the morphological instability, the pattern selected by the system is a fourfold dendrite with the four tips propagating along the coordinate directions. The sudden contraction (or the expansion) of the liquid in front of the interface originates a pressure wave which propagates both into the solid and into the liquid. This effect is illustrated in Figs. 1(a) and 1(c) where the pressure field is shown in the liquid at three different times; the crystal is represented as a black spot at the center of the graph. Here the density ratio is $S=1.05$, and we can clearly observe the large pressure drop in front of the

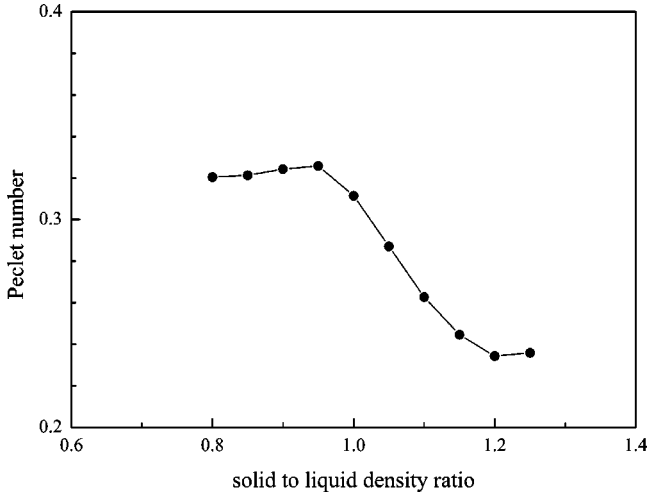

FIG. 3. The Peclet number vs the density ratio S.

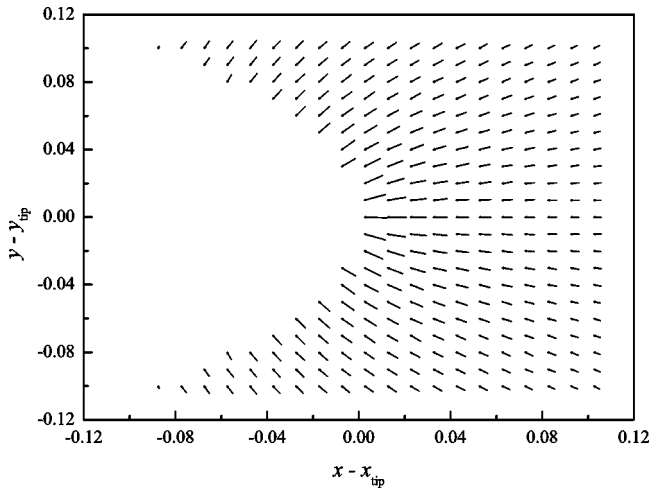

FIG. 4. The flow field in proximity of the dendrite tip, at $t=2.70\times10^{-2}$. The density ratio is $S=1.25$.

dendrite tips. The pressure front reaches the domain's boundaries, where it is reflected and redirected towards the crystal [Fig. 1(b)–1(c)]. At this stage we are far from a steady mechanical regime; nevertheless, the shape of the crystal is already well defined, and we checked that both the tip velocity and the tip radius reached their steady values. A natural question is whether the Peclet number, which in the diffusive picture is only dependent on Δ, is affected by the advection flow driven by the density change. Figures 2 and 3 show the tip velocity, the tip radius and the Peclet number observed in steady conditions at different values of the density ratio S. We note that the heat transported away from (or towards) the interface by the liquid flow in the melt has a strong effect on the growth rate, which decreases with increasing S. On the other hand, R_{tip} increases with S except in a small range between $1.00\leqslant S\leqslant1.10$. The Peclet number is almost constant for $0.80\leqslant S\leqslant0.95$, then decreases with increasing S between $0.95\leqslant S\leqslant1.20$. In this range we have an agreement

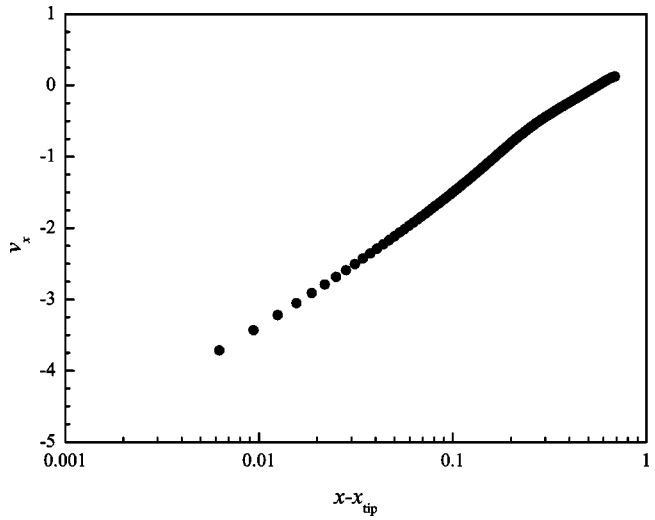

FIG. 5. The liquid velocity on the axis of the dendrite, at $t=2.70\times10^{-2}$. The density ratio is $S=1.25$.

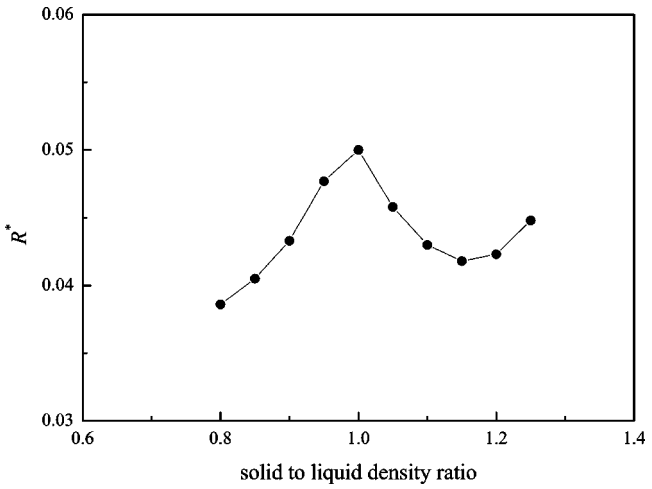

FIG. 6. The instability radius (defined in the text) vs the density ratio *S*.

with the results of McFadden and Coriell [4], obtained with a sharp interface theory without capillary and kinetic effects. Figure 4 shows the flow field in the liquid, in proximity of the dendrite tip. In this case $S=1.25$, and the streamlines converge towards the solid-liquid interface. The extinction of the flow far from the growing crystal is clearly observable. The analysis of McFadden and Coriell [4] shows that in three dimensions the flow decays along the tip axis as $1/d$, where d is the distance from the tip. Thus, the rate of decay is intermediate in order between that for a planar interface, which has a constant flow normal to the interface, and that for a spherical symmetry, for which the flow decays as the square of the distance. We found an analogous result in two dimensions. Figure 5 shows the velocity in the liquid on the x axis, as a function of $d=x-x_{\mathrm{tip}}$. We observe that the dependence $v_x(d)$ is approximately logarithmic, instead of the $v_x \sim d^{-1}$ characteristic for circular growth.

For the pure diffusive problem, the linear analysis of Mullins and Sekerka [10] can determine the largest radius R^* of the crystal which still corresponds to a stable symmetric growth. An interesting question is whether or not the flow in the liquid alters the onset of the morphological instability. A reasonable estimation of R^* may be given as the largest value of the radius of curvature observed along the growth, before the formation of the tip. Figure 6 shows R^* for different values of the density ratio *S*. We may observe that the most stable growth corresponds to the absence of flow in the liquid. The dependence $R^*(S)$ is nonmonotonic and reflects the complex interplay between the density effects and the classic competition of capillary and diffusive effects.

The numerical solutions presented in this paper show to what extent the growth of a free dendrite deviates from the pure diffusive description of Ivantsov when the advection flow effects are taken into account. Both the tip velocity and the tip radius, as well as the Peclet number, depend on the density ratio *S*. Our numerical results give a picture of the process which is in qualitative agreement with the analysis of McFadden and Coriell. The onset of the Mullins-Sekerka morphological instability is slightly anticipated by the flow effects.

[1] G.P. Ivantsov, Dokl. Akad. Nauk SSSR **58**, 56 (1947).
[2] A. Barbieri and J.S. Langer, Phys. Rev. A **39**, 5314 (1989).
[3] M.E. Glicksman, M.B. Koss, and E.A. Winsa, Phys. Rev. Lett. **73**, 573 (1994).
[4] G.B. McFadden and S.R. Coriell, J. Cryst. Growth **74**, 507 (1986).
[5] M. Conti, in *Interface and Transport Dynamics*, edited by H. Emmerich, B. Nestler, and M. Schreckenberg, Lecture Notes in Computational Science and Engineering Vol. 32 (Springer-Verlag, Berlin, 2003).
[6] G. Caginalp and J. Jones, Appl. Math. Lett. **4**, 97 (1991).
[7] D.W. Oxtoby and P.R. Harrowell, J. Chem. Phys. **96**, 3834 (1992).
[8] D.M. Anderson, G.B. McFadden, and A.A. Wheeler, Physica D **135**, 175 (2000).
[9] X. Tong, C. Beckermann, and A. Karma, Phys. Rev. E **61**, R49 (2000).
[10] W.W. Mullins and R.F. Sekerka, J. Appl. Phys. **35**, 444 (1964).